Making corrections to your proof

Please follow these instructions to mark changes or add notes to your proof. You can use Adobe Acrobat Reader (download the most recent version from **https://get.adobe.com**) or an open source PDF annotator.

For Adobe Reader, the tools you need to use are contained in **Annotations** in the **Comment** toolbar. You can also right-click on the text for several options. The most useful tools have been highlighted here. If you cannot make the desired change with the tools, please insert a sticky note describing the correction.

Please ensure all changes are visible via the 'Comments List' in the annotated PDF so that your corrections are not missed.

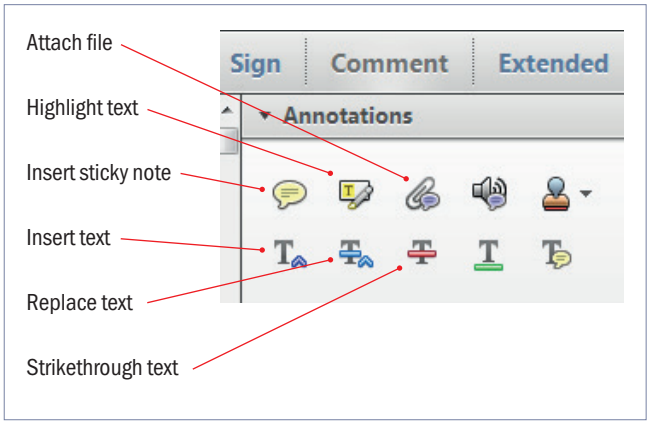

Do not attempt to directly edit the PDF file as changes will not be visible.

Replacing text

To replace text, highlight what you want to change then press the replace text icon, or right-click and press 'Add Note to Replace Text', then insert your text in the pop up box. Highlight the text and right click to style in bold, italic, superscript or subscript.

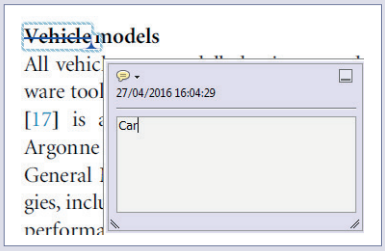

Inserting text

Place your cursor where you want to insert text, then press the insert text icon, or right-click and press 'Insert Text at Cursor', then insert your text in the pop up box. Highlight the text and right click to style in bold, italic, superscript or subscript.

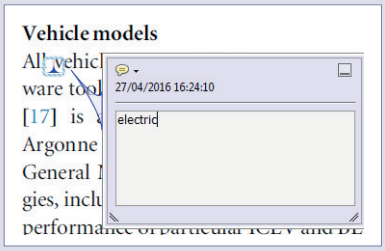

Deleting text

To delete text, highlight what you want to remove then press the strikethrough icon, or right-click and press 'Strikethrough Text'.

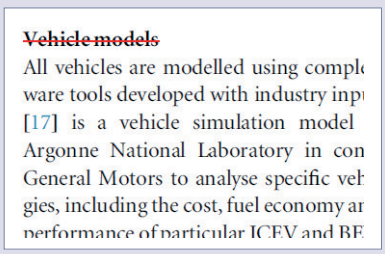

Highlighting text

To highlight text, with the cursor highlight the selected text then press the highlight text icon, or right-click and press 'Highlight text'. If you double click on this highlighted text you can add a comment.

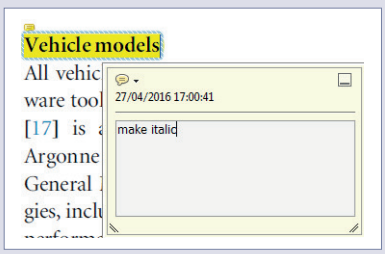

QUERIES

Page 1
AQ1
Your article has been processed in line with the journal style. Your changes will be reviewed by the Production Editor, and any amendments that do not comply with journal style or grammatical correctness will not be applied and will not appear in the published article.
AQ2
Please provide the city name for affiliations [1, 2].
AQ3
Please check that the **names of all authors as displayed in the proof are correct**, and that all **authors are linked to the correct affiliations**. Please also confirm that the correct corresponding author has been indicated. **Note that this is your last opportunity to review and amend this information before your article is published**.
AQ4
Note that the supplementary data associated with your article will be hosted as supplied, and will not be processed by us. If you wish to supply new files, please send them along with your proof corrections.
Page 6
AQ5
Table footnotes [a, b, c] are cited in table 1 but has not been provided. Please remove citation or provide details.
Page 10
AQ6
Please check that the funding information below is correct for inclusion in the article metadata. Fonds Erasme: Bourse Chloé.
AQ7
If an explicit acknowledgment of funding is required, please ensure that it is indicated in your article. If you already have an Acknowledgments section, please check that the information there is complete and correct.
Page 11
AQ8
Please check the details for any journal references that do not have a link as they may contain some incorrect information. If any journal references do not have a link, please update with correct details and supply a Crossref DOI if available.
AQ9
Please provide the volume in Migeotte *et al* (2017).
Page 12
AQ10
Please provide the volume and page/article number details in Taebi and Mansy (2017).
AQ11
Please provide the article title for Taebi *et al* (2019).
AQ12
Please provide the publisher location and name in Zipes *et al* (2018).

Physiological Measurement

IPEM Institute of Physics and Engineering in Medicine

PAPER

Modification of the mechanical cardiac performance during end-expiratory voluntary apnea recorded with ballistocardiography and seismocardiography

RECEIVED
22 June 2019

REVISED
24 September 2019 AQ1

ACCEPTED FOR PUBLICATION
2 October 2019

PUBLISHED

Sofia Morra[1,4,5], Amin Hossein[2], Damien Gorlier[2], Jérémy Rabineau[2], Martin Chaumont[1], Pierre-François Migeotte[2,3] and Philippe van de Borne[1,3]

[1] Department of Cardiology, Erasme Hospital, Université Libre de Bruxelles, [illegible]m AQ2
[2] LPHYS, Université Libre de Bruxelles, [illegible]m
[3] Both authors contributed equally
[4] Author to whom any correspondence should be addressed.
[5] ~~Cardiology Department, Erasme University Hospital, Route de Lennik 808, B-1070, Anderlecht, Brussels, Belgium~~ AQ3

E-mail: sofia.morra@erasme.ulb.ac.be

Keywords: ballistocardiography, seismocardiography, cardio-respiratory interaction, cardiac performance, apnea

Supplementary material for this article is available online

Abstract

Objective. To assess if micro-accelerometers and gyroscopes may provide useful information for the detection of breathing disturbances in further studies. *Methods.* Forty-three healthy volunteers performed a 10 s end-expiratory breath-hold, while ballistocardiograph (BCG) and seismocardiograph (SCG) determined changes in kinetic energy and its integral over time (*i*K, J · s). BCG measures overall body accelerations in response to blood mass ejection into the main vasculature at each cardiac cycle, while SCG records local chest wall vibrations generated beat-by-beat by myocardial activity. This minimally intrusive technology assesses linear accelerations and angular velocities in 12 degrees of freedom to calculate *i*K during the whole cardiac cycle. *i*K produced during systole and diastole were also computed. *Main results.* The *i*K during normal breathing was 87.1 [63.3; 132.8] μJ · s for the SCG and 4.5 [3.3; 6.2] μJ · s for the BCG. Both increased to 107.1 [69.0; 162.0] μJ · s and 6.1 [4.4; 9.0] μJ · s, respectively, during breath-holding ($p = 0.003$ and $p < 0.0001$, respectively). The *i*K of the SCG further increased during spontaneous respiration following apnea (from 107.1 [69.0; 162.0] μJ · s to 160.0 [96.3; 207.3] μJ · s, $p < 0.0001$). The ratio between the *i*K of diastole and systole increased from 0.35 [0.24; 0.45] during apnea to 0.49 [0.31; 0.80] ($p < 0.0001$) during the restoration of respiration. *Significance.* A brief voluntary apnea generates large and distinct increases in SCG and BCG waveforms. *i*K monitoring during sleep may prove useful for the detection of respiratory disturbances. *ClinicalTrials.gov number.* NCT03760159 AQ4

1. Introduction

It is well established that the pulmonary system plays a major role in the modulation of cardiovascular activity. Swings in respiratory-induced pleural pressure rhythmically modify pressure in the inferior vena cava (IVC), pulmonary artery, and across the atria and ventricles and, consequently, blood flow through the cardiac chambers (Pappano and Wier 2013). The pulsus paradoxus reflects this subtle and complex interplay between the cardiovascular and pulmonary systems. A slight fall in systolic blood pressure (SBP) is evident at the peripheral pulses during inspiration. When this fall exceeds 10 mmHg, conditions such as pericardial tamponade, pulmonary embolism, and tension pneumothorax are invoked (Zipes *et al* 2018). Respiratory-induced modifications in peripheral pulse waves reflect corresponding modifications in the interaction between the right and left ventricles. Indeed, the sub-atmospheric pleural pressure generated during inspiration is responsible for a reduction in left ventricle stroke volume (LVSV) secondary to a reduced preload. The reverse is true during expiration (Shuler *et al* 1942, Amit *et al* 2009).

Seismocardiography (SCG) measures low-frequency vibrations produced during a cardiac contractile cycle. These vibrations are transmitted to the chest wall where they generate corresponding specific surface waveforms. Several studies have proposed that certain features obtained from the SCG signals may provide meaningful information regarding heart contractility (Gurev *et al* 2012, Tavakolian *et al* 2012, Jafari Tadi *et al* 2017, Hossein *et al* 2019). Systolic and diastolic times intervals can also be identified on a SCG waveform recording, which allows a cardiac cycle to be split into systolic and diastolic phases (Shafiq *et al* 2016, Jafari Tadi *et al* 2017, Sorensen *et al* 2018).

Ballistocardiography (BCG) is another technique which records, at the body's surface, the vibrations resulting from the recoil forces generated at each cardiac contraction by blood mass ejection.

The BCG waveforms are also profoundly influenced by respiration. The amplitude of the BCG signal increases during spontaneous inspiration and diminishes during spontaneous expiration. The reverse is seen during mechanical ventilation, where the amplitude of the signal diminishes during inspiration (Starr and Friedland 1946). During spontaneous breathing, these respiratory variations appear to depend on changes in intrathoracic pressure which alters blood flow rather than on changes in the heart axis (Starr and Friedland 1946).

The BCG signal is the sum of vibrations coming from both ventricles. It has been proposed however, that the respiratory variations in all BCG waves were similar to those of the right ventricle as it is more affected by respiration than the left ventricle due to its anatomy and position between the cardiovascular and pulmonary system (De Lalla and Brown 1950).

Despite revealing many interesting aspects of cardiovascular physiology and pathology, the popularity of SCG and BCG drastically declined in the mid-90s and they were never incorporated into clinical practice.

These techniques have enjoyed a revival over the past 10 years (Giovangrandi *et al* 2011). Technological advances in micro-accelerometers and gyroscopes sensors have facilitated the development of high-performing portable devices which are user-friendly, thus enabling their deployment in multiple settings from space laboratories (Migeotte *et al* 2016) to the clinical setting. Other techniques are also in development such as, for instance, fiber-optic sensors system by measuring changes in the respiratory rate pattern of patients undergoing MRI examination, to evaluate the degree of anxiety (Dziuda *et al* 2019).

A hybrid model which records BCG and SCG signals at the same time as a one-lead ECG, was developed in 2015 (Migeotte *et al* 2016). This hybrid technique, called kinocardiography (KCG), provides quantitative information on the contractility status of the heart (Hossein *et al* 2019). It allows the simultaneous observation of ballistic and seismic events, including the force of cardiac contraction, the velocity and acceleration of blood mass, and the displacement of the heart axis, and results in corresponding surface waveforms. Specific algorithms (Migeotte *et al* 2016) can use those amplitude signals to derive beat-by-beat scalar parameters, namely the kinetic energy (K, J) and its integral over time (*i*K, J · s) of the cardiac cycle transmitted to the surface sensors as vibratory signals, which result from the movement of both blood and cardiac mass, assuming the cardiovascular system equates with a Newtonian system. Additionally, the *i*K produced during systole and diastole can be computed.

The *i*K is computed on a linear and a rotational channel and their sum equates to the total *i*K (iK_{TOT}). The main content of iK_{TOT} appears to come from the rotational dimension, especially when recorded with the SCG. It accounts for 60% of the total energy and is likely linked to the rotational activity of the blood flow in the aorta and the twisting motion of the heart (Migeotte *et al* 2017).

We have recently demonstrated that the iK_{TOT} recorded with both SCG and BCG accurately estimates dobutamine-induced changes in stroke volume (SV) and cardiac output (CO) in healthy subjects, with a high sensitivity and specificity when compared to echocardiography (Hossein *et al* 2019).

Several studies have been performed to better understand the contribution of respiration to signal genesis of the BCG and SCG (Starr and Friedland 1946, Polo *et al* 1992, Taebi and Mansy 2017). This was possible due to the non-invasive nature of BCG and SCG and the possibility of performing continuous recording. Their relevance in the detection of sleep apnea has also been assessed (Castiglioni *et al* 2012, Wang *et al* 2017).

We aimed to investigate changes in the mechanical activity of the heart recorded with modern micro-accelerations and gyroscopes during normal breathing and voluntary brief end-expiratory apneas. According to the current literature (Starr and Friedland 1946, De Lalla and Brown 1950, Polo *et al* 1992), respiratory-dependent changes of SCG and BCG waveforms are expected. In contrast to previous research, the novelty of this study lies in the ability of micro-acceleration-based technology to quantify respiratory-related changes in cardiac contractile activity measured in terms of *i*K.

2. Methods

2.1. Recruitement and participants

This was a prospective and interventional study.

Forty-nine healthy volunteers were recruited through advertisements among physical education and physiotherapy students at the Université Libre de Bruxelles and Erasme University Hospital, Belgium between October

and December 2018. A medical history was obtained prior to the start of the experimental procedure to rule out any known cardiovascular and/or respiratory disease. None of the subjects took any medication. All participants were informed about the procedure and trained to correctly perform the respiratory maneuvers. All participants gave their informed consent and the study protocol was approved by the local Ethics Committee. The study is registered at ClinicalTrials.gov under the code NCT03760159.

2.2. Haemodynamic and respiratory parameters

Systolic and diastolic blood pressure (SBP, DBP, respectively) and heart rate (HR) were obtained before the beginning of the procedure (sphygmomanometer OMRON 705IT, the Netherlands).

Finger blood pressure was obtained continuously throughout the experimental session using a beat-by-beat haemodynamic monitoring system (Finometer Pro, FMS©, Amsterdam, the Netherlands) and by placing a cuff on the second finger of the right hand. The blood pressure measured with the sphygmomanometer was used as the reference value.

A continuous 3-lead ECG was obtained throughout the whole session.

Oxygen saturation was obtained throughout the session by placing a pulse oximeter on the second finger of the left hand.

Signals were acquired and processed using the data acquisition system PowerLab®16/30 and LabChart® version 5.0 (ADInstruments).

2.3. Kinocardiography

The KCG is a portable system consisting of two modules. The first module (dimension 64 cm^2, weight 104 g) was placed in the lumbar lordosis curve, between the second and the third lumbar vertebrae, close to the subject's center of mass and recorded the BCG signal.

The second module (dimension 24 cm^2, weight 65 g) was placed on the manubrium of the sternum below the clavicle, over the superior mediastinum where the great vessels emerge from the heart. It recorded the SCG signal (see figure 1S (stacks.iop.org/PM/00/0000/mmedia) of supplemental material).

Each module contains a MEMS three-axis accelerometer and three-axis gyroscope sensor (LSM6DSL from STMicroelectronics) and is attached to the body with standard sticky gel electrodes. The KCG is remotely controlled using a smartphone or tablet connected via Bluetooth. It collects a 1-lead ECG at 200 Hz (ADS1292R from AD Instruments) together with 3-degree-of-freedom (DOF) linear (LIN) accelerations and 3-DOF rotational (ROT) angular velocities from the sternum (SCG) and the lumbar region (BCG) (figure 1S of supplemental material). While the BCG measures overall body accelerations in response to the ejection of blood into the main vasculature during each cardiac cycle (Deuchar 1967), the SCG sensor mainly records local chest wall vibrations generated by beat-by-beat myocardial activity (Taebi *et al* 2019). In brief, a total of 12-DOF linear acceleration and angular velocity signals are recorded at 50 Hz. Standard nomenclature was used: for the BCG signal, x is the lateral axis (left-to-right), y is the longitudinal axis (foot-to-head), and z is the antero-posterior axis (ventro-dorsal), while for the SCG signal, the z axis points in the opposite direction (dorso-ventral), x axis is right-to-left, and y axis is the same (figure 1S, supplementary material).

Thanks to an independent component analysis (ICA) of the KCG, it is possible to generate an artificial respiratory signal and to assign each heartbeat to a respiratory phase. Thus, it is possible to detect the inspiratory and expiratory phases of the respiratory cycle (figure 2S, supplementary material). More information on this method has been provided in previous publications (Inan *et al* 2015, Migeotte *et al* 2016, Hossein *et al* 2019).

2.4. Experimental procedure

The procedure consisted of performing end-expiratory apnea for 10 s following maximum exhalation, the lungs being at its residual volume. This maneuver is referred to as 'end-expiratory voluntary apnea' hereafter.

Each apnea was repeated three times, at three-minute intervals.

After attaching the aforementioned instrumentation, the subject was asked to lie motionless on the bed and breath normally. Recordings were performed in the supine position, the upper part of the body at 45°. The quality of signal recorded can be influenced by the body's position (Alametsa *et al* 2008), and this is true mainly for the BCG signal. Sitting and supine positions provide the best BCG signal acquisition capability compared to the standing position (Dziuda and Skibniewski 2014). The supine position was chosen for this study because of technical reasons, mainly to allow complete and correct instrumentation of the volunteer.

Finapress© and ECG were first temporally synchronized, and the record was commenced at the same time as the KCG. After three minutes of normal breathing, the subject was asked to perform the first end-expiratory voluntary apnea. The protocol lasted 10 min and the KCG recording was sent via Bluetooth to the tablet.

Forty-seven out of 49 patients were considered for the analysis: two were excluded because of technical failure during the experimental procedure. Each subject achieved three central apneas; a total of 129 end-expiratory voluntary apneas were obtained. Four records were excluded from the final analysis due to poor signal to noise

ratio, mainly due to motion artifacts. For each subject, the median of the three apneas was considered for further analysis.

2.5. Pre-processing

Powerlab® recordings included ECG, beat-by-beat finger pressure, and oxygen saturation. KCG recordings included independent ECG and linear and rotational SCG and BCG signals. R-peak detection was performed on both KCG and Powerlab® ECG data, and the two generated RR-interval time series were synchronized using a cross correlation technique. This allowed for beat-by-beat correspondence between both data sets for further analysis.

The start and end of the respiratory maneuver were identified manually using the respiratory signal extracted from the KCG as the reference physiological signal. More specifically, the respiratory event coincides with a 'respiratory plateau', where the inspiratory and expiratory phases are no longer identifiable. As such, three 10 s-width windows were obtained for each breathing protocol, each followed by a 10 s-width window of spontaneous breathing referred to as 'recovery'. Using the same method, a 30 s-width window of normal breathing preceding the respiratory event was selected and referred to as 'baseline'. Thirty seconds was chosen for the ensemble average (EA) of the baseline to obtain an average signal independent of the respiratory phase (inspiration or expiration).

Figure 3S of supplementary material shows selection of the respiratory maneuver and its corresponding baseline.

2.6. Signal processing

Data were exported and processed offline using a specific toolbox written in Matlab version 9.5 R2018b (Mathworks®). Further details regarding this methodology have been published previously (Prisk *et al* 2001, Migeotte *et al* 2012, Migeotte *et al* 2016, Hossein *et al* 2019).

P, Q, R, S, and T waves on the ECG were automatically identified and used as reference points for the identification of each cardiac cycle. Individual consecutive SCG and BCG beats, based on automatic identification of the R waves, were averaged over the 10 s-width windows (apnea and recovery) and mean SCG and BCG signals were calculated. These were then used to compute the linear and angular components of the BCG and SCG signals during the respiratory event. The same procedure was applied for the baseline 30 s-width window. This method of sampling and averaging individual beats over a period of time, known as ensemble average (EA), allows a mean BCG and SCG signal to be generated that best represents the shape of a set of cardiac cycles (figure 4S of supplementary material). In addition, this algorithm allows movement-related artifacts to be partially removed. The effects of artifact motion on the recorded signal is shown in figure 5S of supplementary material. This method is explained in detail in Lejeune *et al* (2014).

2.7. *i*K computation for the systolic and diastolic phases of the cardiac cycle

Linear and angular velocities and accelerations are derived from the SCG and BCG signals. Combining these components with parameters of Newtonian mechanics, a series of scalar parameters can be computed. These include K in the linear dimension (K_{LIN}), K in the rotational dimension (K_{ROT}), and total K (K_{TOT}) resulting from the sum of K_{LIN} and K_{ROT}. Temporal integration of K gives the integral of K (*i*K, J · s), which can be computed during systole, diastole, or during the whole cardiac cycle, in both the linear and rotational channels (iK_{LIN}, iK_{ROT}, respectively).

Thanks to the detection of P, Q, R, S and T waves on the ECG, the systolic and diastolic phases are defined as the interval from Q wave to the end of T wave and the interval from the end of T wave to the beginning of the next P wave, respectively.

Figure 1 shows the EA of K_{LIN} and K_{ROT} derived from a SCG signal over a set of contractile cycle.

More details regarding the computation of the above values can be found in (Migeotte *et al* 2016, Hossein *et al* 2019).

2.8. Statistical analyses

Analysis was performed using SPSS IBM® version 22 (SPSS Inc. Chicago, IL).

Categorical variables are presented as counts and percentages.

One-way Friedman's ANOVA for repeated measures was used to compare kinetic energies stratified by respiratory phase (normal breathing, end-expiratory apnea, recovery). The Geisser-Greenhouse correction was considered when Mauchly's test for sphericity was not met. Normality of the difference between pairs was tested using the Kolmogorov-Smirnov test. Pairwise comparison for repeated measures was used to compare each KCG parameter by respiratory phase. Bonferroni correction was applied to account for multiple comparisons, and the corrected *p value* has been set at 0.02. Paired *t* test was used when the data were normally distributed, and Wilcoxon signed rank test was applied to non-normally distributed data.

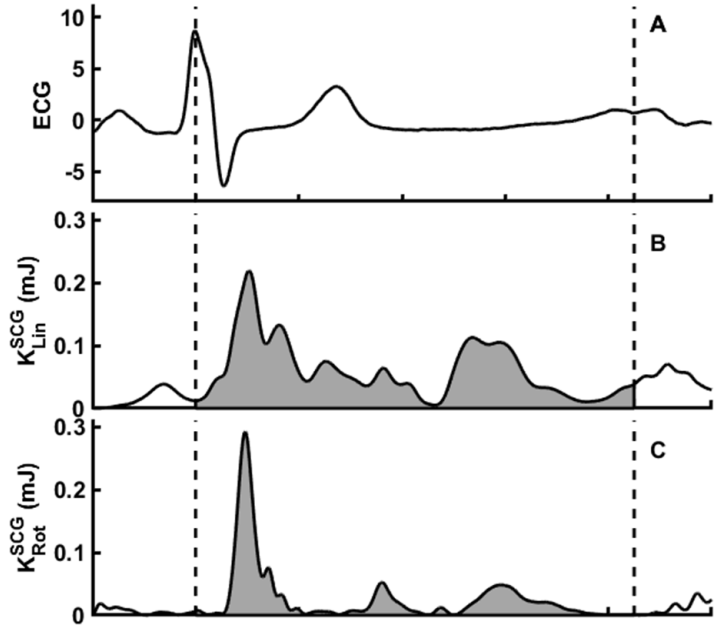

Figure 1. Ensemble average for a set of cardiac cycles obtained from a SCG sensor. From top to bottom: (A) ECG; (B) waveform of K_{SCG} obtained in the linear dimensions; (C) waveform of K_{SCG} obtained in the rotational dimensions. The area under curves B and C represents the computed iK^{SCG}_{Lin} and iK^{SCG}_{Rot}, respectively. The signal between the dashed lines represents the integration process, going from the R peak of the current beat to the beginning of the P wave of the next beat. The continuous vertical line between the dashed lines separates the systolic phase (from the R peak to the end of the T wave) from the diastolic phase (from the end of the T wave to the beginning of the next P wave).

With regards to the beat-by-beat analysis, a linear mixed effect model was applied to the variables.

Results are presented as mean ± Standard Error of the Mean (±SEM) or median and interquantil range [IR] depending on data distribution.

3. Results

Participants were aged 24 ± 0.6 years, had a mean BMI of 22.2 ± 0.4 kg m^{-2}, 57% were female, and 6% were active smokers.

With regards to haemodynamic parameters, HR and $SatO_2$ did not change throughout the respiratory protocol. The mean SBP increased from baseline (121 ± 20 mmHg) to apnea (128 ± 29 mmHg) to recovery (131 ± 29 mmHg) (all $p < 0.004$) The mean DBP however, increased only from apnea (78 ± 13 mmHg) to recovery (82 ± 12 mmHg) ($p < 0.001$).

The *i*K calculated during normal breathing was referred to as 'baseline', while the *i*K calculated during breath-hold and during the 10 s of spontaneous breathing following the end of apnea were referred to as 'end-expiratory voluntary apnea' and 'recovery', respectively.

Table 1 reports total *i*K values computed for both the SCG and the BCG. This includes the sum of the *i*K computed with the linear and rotational channels, namely iK^{SCG}_{Tot}, iK^{BCG}_{Tot}, during the three respiratory phases.

The *i*K of the cardiac cycle, computed using both the SCG and the BCG, increases gradually by approximately 20% for SCG and 35% for BCG from baseline to end-expiratory voluntary apnea and increases further by approximately 60% for SCG and 0% for BCG during recovery compared to end-expiratory voluntary apnea (table 1).

During a normal respiratory cycle only the energy content of the ballistic waves significantly changed from expiratory to inspiratory peaks. The highest value was seen during inspiration rather than expiration (5.8 [4.1; 8.0] $\mu J \cdot s$, 4.6 [3.8; 7.1] $\mu J \cdot s$, $p = 0.009$; table 2).

Moreover, the *i*K produced during brief end-expiratory apnea is higher in magnitude than the one produced during the expiratory peak of a normal respiratory cycle (table 3). Similarly, the *i*K produced during the restoration of respiration following apnea is higher than the one produced during the inspiratory peak of a normal respiratory cycle (table 4).

A marked and significant increase (~50%) of the diastolic energy is evident from apnea to recovery when systolic and diastolic energies are recorded with the SCG (table 1). A significant upward trend is also evident in the systolic energy from apnea to recovery (~25%); however, this is of a lower magnitude than that seen for the diastolic phase. As a result, the ratio between the *i*K of diastole and systole increases significantly (by 40%) during

AQ5 **Table 1.** Variations of the kinetic energy of the contractile cardiac cycle computed with the SCG and BCG and according to the respiratory protocol.

	Normal breathing*	End-expiratory volume, apneab	Recovery	p^{2vs1}	p^{3vs2}	p^{3vs1}
Kinetic energy						
*i*K of SCG	87.1 [63.3; 132.8]	107.1 [69.0; 162.0]	160.0 [96.3; 207.3]	*.003*	*.000*	*.000*
*i*K of BCG	4.5 [3.3; 6.2]	6.1 [4.4; 9.0]	6.2 [3.9; 8.3]	*.000*	.819	*.000*
Kinetic energy of the SCG during systole and diastole						
*i*K systole	57.8 [41.7; 102.5]	74.4 [45.4; 121.3]	92.4 [61.3; 136.2]	*.000*	*.004*	*.000*
*i*K diastole	24.1 [15.1; 38.0]	23.9 [14.4; 31.7]	42.9 [28.2; 60.3]	.782	*.000*	*.000*
*i*K ratio diastole/systole						
*i*K D/S	0.39 [0.30; 0.66]	0.35 [0.24; 0.45]	0.49 [0.31; 0.80]	*.000*	*.000*	*.002*

*i*K: kinetic energy ($\mu J \cdot s$); SCG: seismocardiograph; BCG: ballistocardiograph, *i*K D/S: ratio of the *i*K of the SCG during diastole and systole. Data are expressed as median [IR].

Table 2. Comparison between inspiratory peak and expiratory peak during normal breathing.

	Inspiratory peak	Expiratory peak	*P*
Kinetic energy			
*i*K of SCG	96.5 [70.3; 131.9]	94.7 [67.2; 130.4]	0.267
*i*K of BCG	5.8 [4.1; 8.0]	4.6 [3.8; 7.1]	*0.009*
Kinetic energy of the SCG during systole and diastole			
*i*K systole	58.0 [43.9; 100.6]	60.5 [42.9; 94.9]	0.368
*i*K diastole	24.3 [16.1; 38.2]	23.5 [15.9; 36.8]	*0.05*
*i*K ratio diastole/systole			
*i*K D/S	0.42 [0.26; 0.64]	0.43 [0.29; 0.62]	0.613

*i*K: kinetic energy ($\mu J \cdot s$); SCG: seismocardiograph; BCG: ballistocardiograph, *i*K D/S: ratio of the *i*K of the SCG during diastole and systole.
The date are presented as median [IR].

Table 3. Comparison between expiratory peak during normal breathing and during end-expiratory apnea.

	Expiratory peak	End-expiratory apnea	*p*
Kinetic energy			
*i*K of SCG	94.7 [67.2; 130.4]	107.1 [69.0; 162.0]	*0.02*
*i*K of BCG	4.6 [3.8; 7.1]	6.1 [4.4; 9.0]	*0.003*
Kinetic energy of the SCG during systole and diastole			
*i*K systole	60.5 [42.9; 94.9]	74.4 [45.4; 121.3]	*0.000*
*i*K diastole	23.5 [15.9; 36.8]	23.9 [14.4; 31.7]	0.549
*i*K ratio diastole/systole			
*i*K D/S	0.43 [0.29; 0.62]	0.35 [0.24; 0.45]	*0.000*

*i*K: kinetic energy ($\mu J \cdot s$); SCG: seismocardiograph; BCG: ballistocardiograph, *i*K D/S: ratio of the *i*K of the SCG during diastole and systole. Data are expressed as median [IR].

Table 4. Comparison between inspiratory peak during normal breathing and during the recovery.

	Inspiratory peak	Recovery	*p*
Kinetic energy			
*i*K of SCG	96.5 [70.3; 131.9]	160.0 [96.3; 207.3]	*0.000*
*i*K of BCG	5.8 [4.1; 8.0]	6.2 [4.4; 9.0]	0.655
Kinetic energy of the SCG during systole and diastole			
*i*K systole	58.0 [43.9; 100.6]	92.4 [61.3; 136.2]	*0.000*
*i*K diastole	24.3 [16.1; 38.2]	42.9 [28.2; 60.3]	*0.000*
*i*K ratio diastole/systole			
*i*K D/S	0.42 [0.26; 0.64]	0.49 [0.31; 0.80]	*0.008*

*i*K: kinetic energy ($\mu J \cdot s$); SCG: seismocardiograph; BCG: ballistocardiograph, *i*K D/S: ratio of the *i*K of the SCG during diastole and systole. Data are expressed as median [IR].

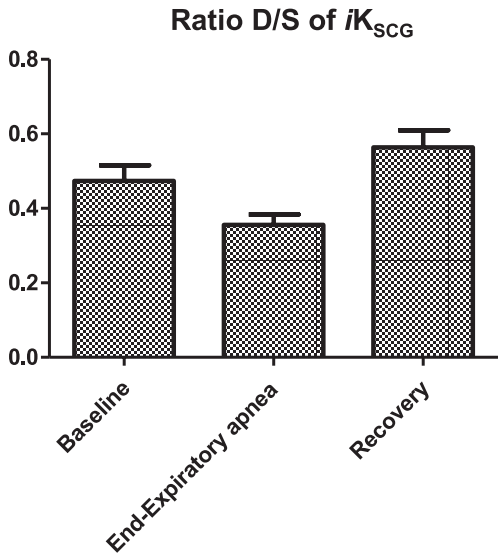

Figure 2. Modification of the ratio of iK_{SCG} computed over diastole and systole according to the respiratory event. Data are presented as mean ± SEM. D, diastole; S, systole.

the restoration of respiration (from 0.35 [0.24; 0.45] to 0.49 [0.31; 0.80], $p = 0.002$). During the transition from baseline to apnea, variations in the energy content during the systolic and diastolic phases are not as remarkable. More specifically, the energy content of systole increases significantly by 35%. The energy of the diastolic phase does not change during breath-hold compared to normal respiration.

Figure 2 illustrates how the ratio between the energy content of diastole and systole changes throughout the respiratory phases.

Table 5 displays the beat-by-beat analysis applied to sixteen beats throughout the respiratory protocol, divided as follows: four beats during normal breathing preceding the beginning of the end-expiratory apnea, four beats following the start of the apnea, four beats before the end of the apnea, and four beats at the beginning of the recovery phase following the end of apnea. At the beginning of apnea, the energy content of a single beat decreased significantly from the first to last beat. This was true for all measurements considered. Conversely, towards the end of apnea, the energy content of a single beat increased from the first to last beat. With regards to the SCG, the *i*K at the beginning of apnea decreased from 210 [125; 271] μJ · s at beat number one to 150 [103; 195] μJ · s at beat number four ($p < 0.001$). On the other hand, the *i*K at the end of apnea increased from 125 [92; 209] μJ · s at beat number one to 233 [135; 413] μJ · s at beat number four ($p = 0.002$). The *i*K of the SCG during systole decreased at the beginning of apnea (from 129 [72; 188] μJ · s at beat number one to 84 [58; 145] μJ · s at beat number four, $p = 0.008$). The *i*K during the diastolic phase decreased at the beginning of apnea (from 43 [29; 70] μJ · s at beat number one to 35 [23; 56] at beat number four, $p = 0.032$). With regards to the BCG, *i*K seems to follow the same trend, even though changes are less significant.

During the recovery phase, the *i*K decreased for all measurements considered. This trend was not statistically significant except for the systolic phase of the SCG, which decreased from 256 [132; 551] μJ · s at beat number one to 163 [107; 333] μJ · s at beat number four ($p = 0.05$), thus going toward the baseline values.

Figure 3 shows the beat-by-beat behavior of the aforementioned parameters throughout the respiratory phases.

4. Discussion

This study shows that the mechanical performance of the heart, recorded with micro-accelerometers and gyroscopes and expressed in terms of *i*K, changes in relation to a specific respiratory event, such as end-expiratory voluntary apnea and the spontaneous inspiration following the breath hold. Also, the systolic and diastolic response to those events is markedly different. Moreover, during the apnea itself, the *i*K evolves from the beginning to the end. These observations are not just a consequence of changes in mechanical coupling due to lung volumes (on SCG) or changes in body inertia (on BCG), as different trends in systole and diastole are clearly visible.

It is already known that BCG and SCG waveforms change according to the respiratory phase, both secondary to variations in blood flow filling the cardiac chambers (Starr and Friedland 1946, Delière *et al* 2015) and lung volume variations (Prisk *et al* 2001). Provided that the KCG can quantify beat-by-beat myocardial contractility

Table 5. Beat-by-beat analysis of all measurements of KCG throughout the respiratory protocol.

	Baseline	Beginning of Apnea	End of Apnea	Recovery
*i*K of SCG	p = ns	$p < 0.001$	$p = 0.002$	p = ns
1	161 [111; 233]	210 [125; 271]	125 [92; 209]	547 [247; 1000]
2	168 [122; 243]	181 [111; 312]	123 [98; 213]	432 [238; 762]
3	171 [110; 225]	142 [110; 253]	146 [109; 240]	361 [243; 682]
4	176 [107; 260]	150 [103; 195]	233 [135; 413]	336 [223; 701]
*i*K systole	p = ns	$p = 0.008$	$p = 0.036$	$p = 0.050$
1	87 [61; 135]	129 [72; 188]	80 [51; 131]	256 [132; 551]
2	87 [65; 136]	124 [75; 208]	83 [56; 149]	235 [118; 450]
3	90 [53; 121]	91 [61; 181]	94 [61; 154]	193 [117; 364]
4	92 [57; 153]	84 [58; 145]	109 [71; 212]	163 [107; 333]
*i*K diastole	p = ns	$p = 0.032$	$p < 0.001$	p = ns
1	45 [35; 72]	43 [29; 70]	37 [26; 64]	137 [75; 214]
2	52 [37; 76]	42 [24; 68]	41 [29; 59]	111 [75; 191]
3	53 [34; 68]	37 [28; 55]	49 [35; 66]	102 [63; 162]
4	54 [29; 89]	35 [23; 56]	79 [47; 176]	95 [51; 173]
*i*K of BCG	$p = 0.006$	$p = 0.057$	$p = 0.056$	p = ns
1	12 [11; 14]	14 [11; 19]	12 [10; 16]	23 [16; 41]
2	12 [10; 15]	15 [11; 20]	13 [10; 16]	17 [14; 27]
3	12 [9; 15]	13 [11; 18]	14 [10; 18]	16 [12; 27]
4	11 [9; 14]	13 [10; 16]	15 [11; 21]	16 [10; 23]

*i*K: integral of kinetic energy (μJ · s); SCG: seismocardiograph; BCG: ballistocardiograph. Data are expressed as median and [IR].

in terms of *i*K (Hossein *et al* 2019), the novelty of the present investigation lies in the dynamic quantification of myocardial contractility during simulated end-expiratory apnea and spontaneous respiratory recovery. In particular, the *i*K increases when the breath is held after maximal expiration, especially at the end of the apnea, and increases further when respiration resumes.

However, the *i*K recorded with the SCG does not change significantly between the expiratory and inspiratory peaks during a normal respiratory cycle, while for the BCG, the magnitude of the *i*K diminishes slightly (20%) from inspiration to expiration (table 2). Despite the small, yet significant difference, our observation is consistent with the one reported by Starr and colleagues (Starr and Friedland 1946). They stated that during expiration, the amplitude of the ballistic waves diminish. Later, Prisk and colleagues observed the same results (Prisk *et al* 2001). In our study however, we did not consider the change in amplitude of waveforms, but rather the change in energy content of a set of cardiac cycles.

The energy content of a set of cardiac cycles produced at the end of normal expiration is not the same as the one produced during short end-expiratory apnea. Indeed, during apnea, the *i*K of both SCG and BCG is greater than that produced during normal expiration (table 3). Similar behavior is seen when normal and deep inspiration following apnea is compared; the *i*K recorded exclusively with the SCG during deep inspiration is higher in magnitude than that recorded during normal inspiration (table 4).

These results suggest that the respiratory event must be of sufficient intensity to impede the cardiovascular system before it becomes detectable with micro-accelerometers and gyroscopes.

The *i*K produced during diastole increases more than the one produced during systole, only when the breathing is restored (table 1). During the recovery phase, the increase in diastolic *i*K is likely linked to increased venous return secondary to the subatmospheric intrathoracic pressure which occurs during deep inspiration. This translates hemodynamically into a larger amount of blood filling the cardiac chambers, specifically the right ventricle (RV), in an acceleration of blood flow returning to the right heart. This subsequently causes an increase in intracardiac filling pressure (Pappano and Wier 2013, Claessen *et al* 2014), likely resulting in a greater *i*K value computed during the diastolic phase. In accordance with Starling's law, the *i*K produced during systole also increases during the recovery phase because of increased cardiac filling. We suggest that modification in the energy content of a set of cardiac cycles seen during spontaneous inspiration subsequent to breath-hold corresponds to modifications in volume in the right heart. The latter increases during inspiration along with its volume (Claessen *et al* 2014), thus concealing simultaneous diminution in the left ventricle (LV) volume (Shuler *et al* 1942).

However, the *i*K also increases during brief end-expiratory apnea compared to normal respiration. We hypothesize that the *i*K recorded at this very respiratory event results from the sum of vector produced by contraction of the left heart, whose volume and size increase during this phase of the cardiac cycle, thus concealing

the simultaneous diminution in the RV volume (Claessen *et al* 2014). An inotropic effect due to activation of the sympathetic system could also be invoked as further explained below.

We also observed that the contribution of systole and diastole to the *i*K of the whole cardiac cycle changed according to the respiratory event. Indeed, the *i*K produced during both systole and diastole increased from normal breathing to apnea to recovery, except for the diastolic *i*K computed during apnea, which did not change compared to normal breathing. The ratio between the diastolic and the systolic energy content decreased during the breath-hold compared to normal breathing and highly increased during spontaneous inspiration following breath-hold, suggesting that the *i*K produced during diastole increases more that the one generated during systole, especially when respiration is restored.

The beat-by-beat analysis provides us with a deep and meaningful insight into the behavior of the KCG measurements for each heartbeat. These results differ slightly from those from the EA analysis, allowing us to go a step further in the interpretation of results. Indeed, the energy content produced by each heartbeat evolves throughout the apnea, showing a decreasing trend at the beginning and an increasing trend at the end. This is true for all the measurements considered. The initial reduction in *i*K observed for the first four beats at the beginning of apnea may be attributable to a transient reduction in the preload which occurs physiologically during expiration (Pappano and Wier 2013), may the apnea be considered a prolonged exhalation. Conversely, the *i*K rises during the four last beats at the end of apnea, possibly due to a progressive rise in sympathetic activity (van de Borne *et al* 1996, Najem *et al* 2006, Heusser *et al* 2009, Breskovic *et al* 2011).

Some readers might argue that the results of the beat-by-beat analysis are not in agreement with the results from the EA analysis; however, they are complementary. The surge of *i*K computed over the whole apneic episode is mainly due to *i*K gradually increasing as apnea ends, overcoming the initial transient reduction. The final result represents a global surge of the *i*K, as the EA analysis shows.

We conclude that during a brief breath-hold and, even more, upon cessation of apnea, there is a marked upsurge in the *i*K produced during a set of contractile cycles. With regards to the apneic phase, the rise in *i*K is likely due to increased *i*K produced during the very last beats at the end of apnea, as shown by the beat-by-beat analysis, and is reasonably related to a rise in sympathetic activity and its haemodynamic consequences.

Moreover, the energy content of the ballistic waveforms also changes between the inspiratory and the expiratory peaks, reaching the highest values during inspiration. When using a SCG, however, the energy content of a set of cardiac cycles are similar between the inspiratory and expiratory peaks during normal breathing, suggesting that the respiratory event must be of significant intensity to induce significant modifications of the SCG parameters.

4.1. Limitations

Some important limitations need consideration. Despite being conducted under standardized conditions and following instruction of the experimenter, performing an apnea is dependent on the subject's collaboration. Additionally, it was critical for the subject to stay as motionless as possible to avoid motion artifacts and for the accelerometric record of the KCG to be reliable.

Volunteers have all been recruited among physical education and physiotherapy students at the Erasme University Hospital and at the Université Libre de Bruxelles. Readers may consider this as a selection bias, however the present study was conceived to be applied to healthy individuals. Indeed, anthropometric parameters such as BMI and age may strongly influences the signals recorded with SCG and BCG, so that similar conclusions could probably not be secured in case of different BMI and/or age.

The impact of BMI age on the ballistic and seismic signals will be the object of a forthcoming study.

As explained above (paragraph 2.3), the first module is placed over the lumbar lordosis and the second one on the manubrium of the sternum. Authors took great care in placing modules on the skin surface of the subject, and always took anatomic structures as reference to place them correctly. Authors believe that the different arrangement of the boxes on different test days does not change the results (preliminary observations from unpublished studies).

Sensors could have also been placed on the bed where the experimental session took place, in order to minimize the staff participation and to reduce the risk of failing the right anatomical position. However, sensors placed on the bed records only the ballistic waves while recording of the seismocardiographic signal need the sensor to be placed close to the heart, which is impractical if the sensors are placed on the bed.

The current study has not considered the heart rate variability (HRV) analysis extracted from the BCG and how it may be influenced by the apnea. HRV is indeed an important clinical marker to quantitative evaluate the autonomic activity, which is strongly associated with cardiovascular mortality, including sudden cardiac death (SCD), particularly in older individuals. With the advent of highly performing BCG systems and improvement of technology, HRV may also be extracted from the BCG signals, specifically from the J–J interval (Gonzalez-Landaeta *et al* 2007, Wang *et al* 2015), which represents a good surrogate of the RR interval. Comparing the BCG and ECG extracted HRV during normal breathing and the apnea could be the object of further investigations.

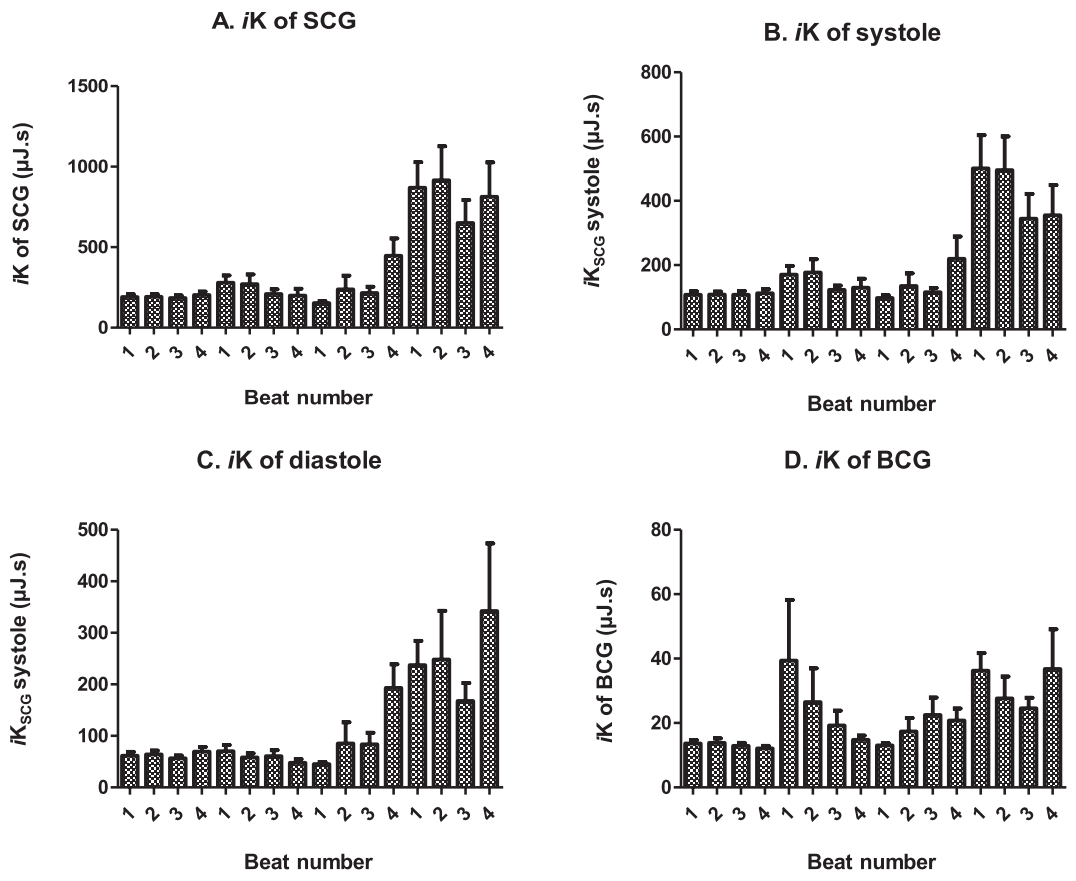

Figure 3. Representation of *i*K computed with the SCG and BCG beat by beat. Panels display from the above downward and from left to right: A. *i*K of the SCG, B. *i*K of the systole computed from the SCG waveforms, C. *i*K of diastole computed from the SCG waveforms; D. *i*K of BCG. A total of sixteen consecutive beats have been computed and analyzed throughout the respiratory protocol. Beats were clustered according to the respiratory phase as follow: the first group 1 to 4 are the first four beats before the beginning of the apnea; the second group 1 to 4 are the first four beats after the beginning of the apnea; the third group 1 to 4 are the last four beats of the apnea; the fourth group 1 to 4 are the first four beats after the end of the apnea. Data are presented as mean (±SEM). *i*K, integral of kinetic energy; SCG, seismocardiography; BCG, ballistocardiography.

Another limitation is that the activity of the sympathetic system was not recorded in this study. Thus, the hypothesis that a rise in sympathetic activity at the end of apnea causes the observed phenomenon remains speculative, even though SBP increased concomitantly. The duration of apnea in our study was only 10 s and did not result in a noticeable reduction in O_2 saturation. Thus, a large rise in sympathetic activity during apnea is also unlikely.

Finally, KCG signals should be examined and conclusions drawn carefully, as the genesis of SCG and BCG signals is complex and involves multiple systemic and local phenomena.

5. Conclusions

Provided that the underlying assumptions and limitations of the SCG and BCG are acknowledged, we can gain a new physiological insight into cardiac mechanics, expressed in terms of *i*K, during simulated end-expiratory apnea and subsequent spontaneous inspiration. Specifically, the *i*K produced within a set of cardiac cycles changes significantly according to the respiratory event and, in terms of the ballistic waves, also changes significantly between the inspiratory and expiratory phases of a normal breathing cycle. The respective contribution of hemodynamic changes, organ displacements, and related changes in autonomic activity are at present speculative. Further research is however warranted in this area, especially as we observed large and distinct increases in SCG and BCG generated by a brief voluntary apnea, suggesting that *i*K monitoring during sleep may prove useful for the detection of respiratory disturbances.

AQ6 ## Acknowledgments

AQ7 The authors would like to acknowledge the contribution of the volunteers and staff members of the Cardiology Department of the Erasme-Hospital. We thank Mme Lise Mathelet for active participation in the recruitment of

volunteers and Mr. Olivier Van Hove for providing us with the spirometer. We want to thank the Fonds Erasme foundation for promoting this research project.

Grants

This work was supported by the 'FONDS ERASME pour la recherche médicale; Bourse Chloé' of the Erasme hospital, Bruxelles, Belgium.

Disclosures

Authors do not declare any conflict of interest.

Authors contributions

SM and PVDB conceived the idea and design of the study. SM carried out the whole experimental procedure, from the recruitment of volunteers to conducting the experimental session. SM had full access to all data in the study and takes responsibility for the integrity of the data and the accuracy of the data analysis. PFM, AH, JR and DG developed the signal processing algorithms for the ECG and KCG signals. AH was responsible for the extrapolation of all metrics from KCG records as well as for their synchronization with signals of Finapress© and Capnostream®. SM, JR and AH performed the statistical analysis. SM drafted the manuscript. AH, JR, DG, MC, PFM and PVDB revised the manuscript critically for important intellectual content. All the authors proofread and made corrections to this manuscript.

AQ8

References

Ä[illegible]sa J, Viik J, Alakare J, Varri A and Palomaki A 2008 Ballistocardiography in sitting and horizontal positions *Physiol. Meas.* **29** 1071–87

Amit G, Shukha K, Gavriely N and Intrator N 2009 Respiratory modulation of heart sound morphology *Am. J. Physiol. Heart Circ. Physiol.* **296** H796–805

Breskovic T, Steinback C D, Salmanpour A, Shoemaker J K and Dujic Z 2011 Recruitment pattern of sympathetic neurons during breath-holding at different lung volumes in apnea divers and controls *Auton. Neurosci.* **164** 74–81

Castiglioni P *et al* 2012 Seismocardiography while sleeping at high altitude *Conf. Proc. IEEE Engineering in Medicine and Biology Society* vol 2012 pp 3793–6

Claessen G, Claus P, Delcroix M, Bogaert J, La Gerche A and Heidbuchel H 2014 Interaction between respiration and right versus left ventricular volumes at rest and during exercise: a real-time cardiac magnetic resonance study *Am. J. Physiol. Heart Circ. Physiol.* **306** H816–24

De Lalla V Jr and Brown H R Jr 1950 Respiratory variation of the ballistocardiogram *Am. J. Med.* **9** 728–33

Delière Q, Tank J, Funtova I, Luchitskaya E, Gall D, van de Borne P and Migeotte P F 2015 Ballistocardiogram amplitude modulation induced by respiration: a wavelet approach *Comput. Cardiol.* **42** 313–6

Deuchar D C 1967 Ballistocardiography *Br. Heart J.* **29** 285–8

Dziuda L S and Skibniewski F W 2014 A new approach to ballistocardiographic measurements using fibre Bragg grating-based sensors *Biocybernetics Biomed. Engi.* **34** 101–16

Dziuda L, Zielinski P, Baran P, Krej M and Kopka L 2019 A study of the relationship between the level of anxiety declared by MRI patients in the STAI questionnaire and their respiratory rate acquired by a fibre-optic sensor system *Sci. Rep.* **9** 4341

Giovangrandi L, Inan O T, Wiard R M, Etemadi M and Kovacs G T 2011 Ballistocardiography—a method worth revisiting *Conf. Proc. IEEE Engineering in Medicine and Biology Society* vol 2011 pp 4279–82

Gonzalez-Landaeta R, Casas O and Pallas-Areny R 2007 Heart rate detection from an electronic weighing scale *Conf. Proc. IEEE Engineering in Medicine and Biology Society* vol 2007 pp 6283–6

Gurev V, Tavakolian K, Constantino J, Kaminska B, Blaber A P and Trayanova N A 2012 Mechanisms underlying isovolumic contraction and ejection peaks in seismocardiogram morphology *J. Med. Biol. Eng.* **32** 103–10

Heusser K *et al* 2009 Cardiovascular regulation during apnea in elite divers *Hypertension* **53** 719–24

Hossein A, Mirica D C, Rabineau J, del Rio J I, Morra S, Gorlier D, Nonclercq A, van de Borne P and Migeotte P F 2019 Accurate detection of dobutamine-induced haemodynamic changes by kino-cardiography: a randomized double-blind placebo-controlled validation study *Sci. Rep.* **9** 10479

Inan O T *et al* 2015 Ballistocardiography and seismocardiography: a review of recent advances *IEEE J. Biomed. Health Inform.* **19** 1414–27

Jafari Tadi M *et al* 2017 Gyrocardiography: a new non-invasive monitoring method for the assessment of cardiac mechanics and the estimation of hemodynamic variables *Sci. Rep.* **7** 6823

Lejeune L, Caiani E G, Prisk G K and Migeotte P F 2014 Evaluation of ensemble averaging methods in 3D ballistocardiography *Conf. Proc. IEEE Engineering in Medicine and Biology Society* vol 2014 pp 5176–9

Migeotte P F *et al* 2012 Three dimensional ballisto- and seismo-cardiography: HIJ wave amplitudes are poorly correlated to maximal systolic force vector *Conf. Proc. IEEE Engineering in Medicine and Biology Society* vol 2012 pp 5046–9

Migeotte P F, Monfils J, Landreani F, Funtova I I, Tank J, van de Borne P and Caiani E G 2017 P439 Cardiac strength deconditioning after the 60-days head-down bed-rest assessed by heart kinetic energy wearable monitoring *Eur. Heart J.* 38 AQ9

Migeotte P F, Mucci V, Delière Q, Lejeune L and van de Borne P 2016 Multi-dimensional kinetocardiography a new approach for wearable cardiac monitoring through body acceleration recordings *XIV Mediterranean Conf. on Medical and Biological Engineering and Computing* pp 1125–30

Najem B *et al* 2006 Acute cardiovascular and sympathetic effects of nicotine replacement therapy *Hypertension* **47** 1162–7

Pappano A J and Wier G W 2013 Control of cardiac output: coupling of heart and blood vessels *Cardiovascular Physiology* 10th edn (New York: Elsevier) pp 195–222

Polo O, Tafti M, Hamalainen M, Vaahtoranta K and Alihanka J 1992 Respiratory variation of the ballistocardiogram during increased respiratory load and voluntary central apnoea *Eur. Respir. J.* **5** 257–62

Prisk G K, Verhaeghe S, Padeken D, Hamacher H and Paiva M 2001 Three-dimensional ballistocardiography and respiratory motion in sustained microgravity *Aviat Space Environ. Med.* **72** 1067–74

Shafiq G, Tatinati S, Ang W T and Veluvolu K C 2016 Automatic Identification of Systolic Time Intervals in Seismocardiogram *Sci. Rep.* **6** 37524

Shuler R H, Ensor C, Gunning R E, Moss W G and Johnson V 1942 The differential effects of respiration on the left and right ventricles *Am. J. Physiol.* **137** 620–7

Sorensen K, Schmidt S E, Jensen A S, Sogaard P and Struijk J J 2018 Definition of fiducial points in the normal seismocardiogram *Sci. Rep.* **8** 15455

Starr I and Friedland C K 1946 On the cause of the respiratory variation of the ballistocardiogram, with a note on sinus arrhythmia *J. Clin. Invest.* **25** 53–64

Taebi A and Mansy H A 2017 Grouping similar seismocardiographic signals using respiratory information *IEEE J. Biomed. Health Inform.* AQ10

Taebi A, Solar B E, Bomar A J, Sandler R H and Mansy H A 2019 *Recent Adv. Seismocardiogr. Vib.* **2** 64–86 AQ11

Tavakolian K *et al* 2012 Myocardial contractility: a seismocardiography approach *Conf. Proc. IEEE Engineering in Medicine and Biology Society* vol 2012 pp 3801–4

van de Borne P, Oren R, Anderson E A, Mark A L and Somers V K 1996 Tonic chemoreflex activation does not contribute to elevated muscle sympathetic nerve activity in heart failure *Circulation* **94** 1325–8

Wang K *et al* 2015 Comparison of heart rate variability measurements between ballistocardiogram and electrocardiography *Zhonghua Xin Xue Guan Bing Za Zhi* **43** 448–51

Wang Z, Zhou X, Zhao W, Liu F, Ni H and Yu Z 2017 Assessing the severity of sleep apnea syndrome based on ballistocardiogram *PLoS One* **12** e0175351

Zipes D P, Libby P, Bonow R O, Mann D L and Tomaselli G F 2018 *Braunwald's Heart Disease: a Textbook of Cardiovascular Medicine* 11th AQ12 edn